Biosensors and Bioelectronics 100 (2018) 228–234

Contents lists available at ScienceDirect

Biosensors and Bioelectronics

journal homepage: www.elsevier.com/locate/bios

Highly sensitive surface plasmon resonance biosensor for the detection of HIV-related DNA based on dynamic and structural DNA nanodevices

Wei Diao[1], Min Tang[1], Shijia Ding, Xinmin Li, Wenbin Cheng, Fei Mo, Xiaoyu Yan, Hongmin Ma, Yurong Yan*

Key Laboratory of Clinical Laboratory Diagnostics (Ministry of Education), College of Laboratory Medicine, Chongqing Medical University, Chongqing 400016, China

ARTICLE INFO

Keywords:
HIV-related DNA
Surface plasmon resonance
DNA nanodevice
Entropy-driven strand displacement reaction
Double-layer DNA tetrahedron
Biosensing strategy

ABSTRACT

Early detection, diagnosis and treatment of human immune deficiency virus (HIV) infection is the key to reduce acquired immunodeficiency syndrome (AIDS) mortality. In our research, an innovative surface plasmon resonance (SPR) biosensing strategy has been developed for highly sensitive detection of HIV-related DNA based on entropy-driven strand displacement reactions (ESDRs) and double-layer DNA tetrahedrons (DDTs). ESDRs as enzyme-free and label-free signal amplification circuit can be specifically triggered by target DNA, leading to the cyclic utilization of target DNA and the formation of plentiful double-stranded DNA (dsDNA) products. Subsequently, the dsDNA products bind to the immobilized hairpin capture probes and further combine with DDTs nanostructures. Due to the high efficiency of ESDRs and large molecular weight of DDTs, the SPR response signal was enhanced dramatically. The proposed SPR biosensor could detect target DNA sensitively and specifically in a linear range from 1 pM to 150 nM with a detection limit of 48 fM. In addition, the whole detecting process can be accomplished in 60 min with high accuracy and duplicability. In particular, the developed SPR biosensor was successfully used to analyze target DNA in complex biological sample, indicating that the developed strategy is promising for rapid and early clinical diagnosis of HIV infection.

1. Introduction

Acquired immunodeficiency syndrome (AIDS) with high mortality is a common infectious disease caused by the human immune deficiency virus (HIV). Early diagnosis and therapy of HIV infection can effectively protect the host's immune functions and prolong survival period (Girardi et al., 2007). The common methods for clinical diagnosis of HIV infection, including enzyme-linked immunosorbent assay (ELISA) and western blot (WB), are unable to identify the early stage of infection due to low HIV antibody levels (De la Rica and Stevens, 2012; Zhou et al., 2015). Polymerase chain reaction (PCR)-based techniques are sensitive and reliable but require thermal cycling and complicated primer design (Avettand-Fenoel et al., 2009). Therefore, it is highly desirable to develop simple, rapid and isothermal techniques to realize the early diagnosis of HIV infection.

As alternatives to conventional methods, various biosensing techniques have been developed for HIV-related DNA detection, such as electrochemistry (Wang et al., 2015), colorimetry (Long et al., 2016), fluorescence resonance energy transfer (FRET) (Qaddare and Salimi, 2017), and surface plasmon resonance (SPR) (Wu et al., 2007) etc. Among them, SPR biosensing is a powerful analytical tool due to its obvious advantages of stable, label-free, real-time monitoring and analysis. The SPR response signal has high relevance to the weight of molecules bound to the chip surface. Up to now, a number of modern SPR assays employ enzyme-based signal amplification strategies (Miao et al., 2016; Xiang et al., 2015; Yao et al., 2015) or metallic nanomaterials (Hao et al., 2017; Wang et al., 2016; Yuan et al., 2017) to improve the sensitivity. However, enzyme-based signal amplification strategies have some major shortcomings, including easy loss of catalytic activity, high cost, and harsh reaction conditions. In addition, the synthesis of metallic nanomaterials suffers from complicated procedure and poor controllability. At the same time, the DNA coverage on metallic nanomaterials surface may cause lower hybridization efficiency due to local overcrowding effect (Pei et al., 2012). Fortunately, DNA nanotechnology offers new approach to address the above problems.

DNA nanotechnology utilizing DNA strands to manipulate the spatial and temporal distribution of matter can construct various

* Corresponding author.
E-mail address: yanyurong163@163.com (Y. Yan).
[1] These authors contributed equally to this work.

http://dx.doi.org/10.1016/j.bios.2017.08.042
Received 14 June 2017; Received in revised form 9 August 2017; Accepted 17 August 2017
Available online 09 September 2017
0956-5663/ © 2017 Elsevier B.V. All rights reserved.

dynamic and structural DNA nanodevices with high precision and excellent controllability (Zhang and Seelig, 2011). Dynamic DNA nanodevices such as hybridization chain reaction (HCR) (Ding et al., 2017; Wu et al., 2016), catalytic hairpin assembly (CHA) (Li et al., 2016c, 2016b) and entropy-driven strand displacement reactions (ESDRs) (Li et al., 2015; Wu et al., 2014), have been used for the design of simple and enzyme-free assay approaches to achieve highly sensitive detection of analytes. As an isothermal and high-efficiency signal amplification technique with negligible background, ESDRs have grown into a promising strategy for DNA detection. ESDRs are driven forward by exclusive entropy force with superior features, such as flexible sequence design, excellent thermostability, and robust resistance to complex environments. Owing to the programmability and versatility, ESDRs-based signal amplification technique has been applied to the construction of various biosensing systems (Feng et al., 2017; Lv et al., 2015; Shi et al., 2015).

On the other hand, structural DNA nanodevices of varying dimensions, shapes, and geometries have been successfully assembled, such as DNA nanotube (Douglas et al., 2007), DNA nanoflower (Zhu et al., 2013), and DNA tetrahedron (Goodman et al., 2005), etc. Especially, three-dimensional DNA tetrahedron, which has excellent mechanical rigidity and structural stability, has attracted considerable research attention in the field of biosensing (He et al., 2017; Liu et al., 2015; Mao et al., 2016). For instance, DNA tetrahedron-decorated gold surfaces or glass substrates have been used to construct biosensors for the detection of DNA/RNA, small-molecule and protein (Lin et al., 2016). Nevertheless, DNA tetrahedron has a complicated fabrication process because its strands require additional chemical modification (Li et al., 2014). To circumvent this problem, DNA tetrahedron can be used as macromolecular biomaterial due to its intrinsic property of high molecular weight without other modifications. Inspired by dendritic DNA nanostructures (Xie et al., 2016), constructing double-layer DNA tetrahedrons (DDTs) can further increase the molecular weight, making DDTs more valuable. Moreover, DNA tetrahedron can reduce the hindrance effect with well-defined spacing and enhance spatial position range, leading to higher hybridizing efficiency (Lin et al., 2015). Hence, ESDRs and DDTs nanostructure can be perfectly applied to SPR biosensing platform for highly sensitive detection of target DNA.

Herein, a highly sensitive SPR biosensing strategy was developed for enzyme-free and label-free HIV-related DNA detection based on DNA nanotechnology of dynamic ESDRs and structural DDTs nanodevices. In this system, hairpin probes were immobilized on the SPR sensor chip surface in advance. The target DNA could bind to the terminal toehold region of three-stranded complexes and initiate toehold-mediated strand displacement reactions, leading to the reuse of target DNA and the production of plentiful double stranded complex. Then, the generated double-stranded complex could specifically hybridize with hairpin probes, exposing the binding sites of DDTs. After the successful capture of DDTs nanostructure, three-decker composites were formed on SPR sensor chip, which amplified the SPR response signal significantly. Therefore, a rapid and isothermal biosensing strategy was achieved for the detection of HIV-related DNA. Compared with the conventional methods, our method can be accomplished in 60 min which shortens the detection time effectively. And HIV-related DNA detection does not rely on the production of antibody, which can efficiently narrow the window period. Compared with other sensing strategies, the proposed strategy can be carried out without any enzymes or complex chemical modification, making the system simple, low-cost and practical. In addition, the proposed strategy enables real-time detection of HIV-related DNA with good stability due to the unique advantages of SPR. In general, the developed dynamic and structural DNA nanodevices provide a promising tool to construct enzyme-free and high capturing efficiency SPR detection strategy for a variety of biomarkers.

2. Experiment section

2.1. Materials and reagents

DNA oligonucleotides were synthesized and purified by Sangon Inc. (Shanghai, China). The base sequences are displayed in Table S1 (Supporting information). All oligonucleotides were dissolved in TE buffer (10 mM Tris HCl, 1 mM EDTA, pH 8.0) and kept at −20 °C. DL500 DNA marker was purchased from Takara (Dalian, China). GoldView was purchased from SBS Genetech (Beijing, China). ESDRs buffer (pH 7.0) comprised 10 mM Tris, 480 mM NaCl, and 5 mM $MgCl_2$. DNA tetrahedral assembly buffer (TM buffer, pH 8.0) comprised 20 mM Tris and 50 mM $MgCl_2$. Running buffer (pH 7.4) comprised 30 mM sodium phosphate, 450 mM NaCl, 3 mM EDTA, and 0.25% Triton×100. All other reagents were of analytical grade, and Milli-Q water (≥ 18 MΩ) was utilized in every test.

2.2. Apparatus

Biacore X™ analytical system (Biacore AB, Uppsala, Sweden) and bare gold sensing chips (SIA kit Au) were utilized in the SPR measurement. For all the experiments, the flow rate of the SPR system was set to 2 μL min^{-1}. The Biacore X™ shows outcomes as a time course of resonance units (RU). Every sensorgram was exhibited and assessed with the BIA evaluation 4.1 software (Biacore, Sweden). The gel electrophoresis was conducted on DYY-6C electrophoresis analyzer (Liuyi Instrument Company, China) and visualized on Bio-Rad ChemDoc XRS (Bio-Rad, USA). Atomic force microscope (AFM) Dimension Icon (Bruker AXS, Germany) was employed to characterize the size and morphology of DNA tetrahedron nanostructure.

2.3. Preparation of probes

The sequence of HIV-related DNA was designed based on journal publications (Wang et al., 2015; Zhou et al., 2014). DNA sequences of ESDRs amplification system and DDTs nanostructure were designed referring to recently published work (Lv et al., 2015; Lin et al., 2016). Before using, the hairpin capture probes were denatured at 95 °C for 5 min and chilled to room temperature gradually. The three-stranded beacon complexes of ESDRs were prepared with single strand Q, P and R at 1:1.2:1.2 M ratio in ESDRs buffer. The solution was heated to 95 °C for 5 min and chilled to room temperature gradually. Then the probes were kept at 4 °C for further use.

2.4. Preparation of DNA tetrahedron nanostructures

The DDTs nanostructure was prepared through the successive assembly of monomers DNA tetrahedrons according to the reference. Two types of tetrahedron DNA monomers T_0 and T_1 were synthesized in advance using same process to construct DDTs. For the assembly of T_0, single strands a, b, c and d were mixed in equimolar ratio in TM buffer with a final concentration of 1 μM. The solution was heated to 95 °C for 10 min and then chilled to 4 °C gradually to obtain monomers T_0. One sticky end of T_0 could hybridize with surface-confined dsDNA product of ESDRs, and the other three same sticky ends could hybridize with T_1. After assembly, mix T_0 up with T_1 at a 1:3 ratios and further incubated for 1 h at 37 °C to form DDTs nanostructure. DDTs can be stored at 4 °C for at least 1 week for further use.

2.5. Preparation of SPR biosensor

The hairpin capture probes were immobilized on the gold sensing chip via Au–S bond. The chip surface was first cleansed using newly prepared piranha solution (30% H_2O_2, 70% H_2SO_4) for 10 min to eradicate other elements, then washed completely using ultrapure water and dehydrated at room temperature. Then, the chip was entered

into the Biacore X™ device, and ultrapure water was utilized as running solution. Until the baseline arrived at a stable state, 1 μM hairpin capture probes in immobilization solution (1 M KH_2PO_4, pH 3.8) were injected into the flow cell and reacted for 30 min. After the baseline had restored stability, the running buffer was changed from ultrapure water to SPR running buffer. Then, the chip was prepared for further experiment with no need for blocking with 6-Mercapto-1-hexanol (MCH) (Li et al., 2016a).

The ESDRs amplification system comprised three-stranded complexes (QPR), fuel strand (F) as well as different concentrations of target DNA in ESDRs buffer with the eventual volume of 100 μL. The complexes QPR and fuel strand reached a final concentration of 250 nM. The reaction solution was incubated at 37 °C for 30 min. The sensing chip functionalized with hairpin capture probes were utilized for DNA detection. After the sensorgram had reached a stable status, the prepared reaction solution was infused into the flow cell and moved for 15 min. Subsequently, the solution of 1 μM DDTs nanostructure in TM buffer was infused and moved through the flow-cell for 15 min. Afterwards, the chip was cleansed using running buffer. After each detection process, the chip surface was restored with 50 mM NaOH to eliminate the binding analytes on the gold film and cleansed using running buffer for the next detection. Three repeated tests were implemented to the same sample and the mean result was utilized for computation. The binding/restoration procedures on the same chip were replicated 100 times to evaluate the reusability of the sensing chip.

2.6. Gel electrophoresis

To confirm the usability of DDTs nanostructure, the products and components of DDTs were studied with 8% native polyacrylamide gel electrophoresis (PAGE) in 1×TBE buffer (89 mM Tris-boric acid, 2 mM EDTA, pH 8.3) at a 80 V constant voltage for 100 min. The gels were imaged using gel image system (Bio-Rad Laboratories, USA).

3. Results and discussion

3.1. Design principle of the SPR biosensor

The principle for SPR detection of HIV-related DNA based on ESDRs amplification and DDTs nanostructure is illustrated in Scheme 1.

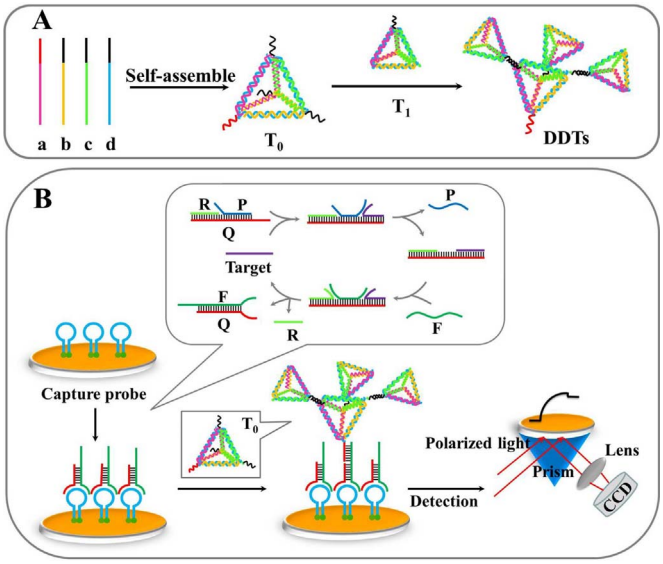

Scheme 1. (A) Schematic illustration of the preparation of DDTs nanostructure; (B) Schematic representation of SPR biosensing strategy for HIV-related DNA detection based on ESDRs and DDTs nanostructure.

Hairpin capture probes are immobilized on the chip surface via Au-S binding in one step and keep appropriate conformation without the need of blocking with MCH. The capture probe consists two parts: the stem part serves as rigid support to keep it upright, and the loop part provides an enclosed platform for dsDNA product F-Q binding. The sequence and structure of capture probe are shown in Fig. S1. Single strand Q, P and R are primarily denatured together to obtain stable three-stranded beacon complexes QPR. The target can specifically bind to the toehold region at 3′-terminus of strand Q and displace strand P through entropy-driven strand displacement reaction. The dissociation of strand P causes the exposure of initially obstructed toehold in the middle of strand Q. Subsequently, the newly exposed toehold can hybridize with strand F, resulting in the liberation of target DNA as well as strand R at the same time. Consequently, the target DNA is utilized again and plenty of dsDNA products F-Q are generated to specifically combine with capture probes. Then with the interaction of dsDNA F-Q and capture probes, the binding site of DDTs is available on the chip surface. Favorably, the prepared DDTs nanostructure can specifically bind to sensor chip generating significantly amplified SPR signal.

A representative SPR sensorgram is described in Fig. 1. ΔRU1 presents the reaction of the hybridization of dsDNA F-Q with capture probes. ΔRU2 presents the reaction of capture probes-F-Q complexes combined with DDTs nanostructures. Thus, the total response of each test is (ΔRU1 + ΔRU2). After the test, the surface can be thoroughly restored using the NaOH (50 mM) solution and cause the dynamic curve back to the baseline for the next sensing.

3.2. Feasibility of the biosensing strategy

The feasibility of the developed amplification strategy for target DNA detection was confirmed by fluorescent and SPR biosensing platforms. Fluorescent platform was first used to confirm whether or not the target DNA triggered the ESDRs amplification reaction. A fluorescent dye (FAM) was labeled at the 5′ end of strand R and a quencher (BHQ-1) was labeled at the 3′ end of strand Q. As shown in Fig. 2A, when the three-stranded complex QPR was formed, the FAM fluorescence was quenched efficiently, showing a negligible fluorescence signal with the value of 54 a.u. (curve d). In the presence of target DNA and fuel strand F, the three-stranded complex was converted to a double-stranded product F-Q releasing report strand R. Meanwhile, target DNA was regenerated to trigger an additional cycle. Thus, a notably high fluorescence signal of 712 a.u. was obtained (curve a). In the absence of target (curve b) or fuel strand F (curve c), only very weak fluorescence signals were obtained with the values of 61 and 66 a.u. respectively. Because ESDRs cannot be carried out owing to the lack of necessary component. The results of fluorescence effectively demonstrated the viability of ESDRs amplification strategy.

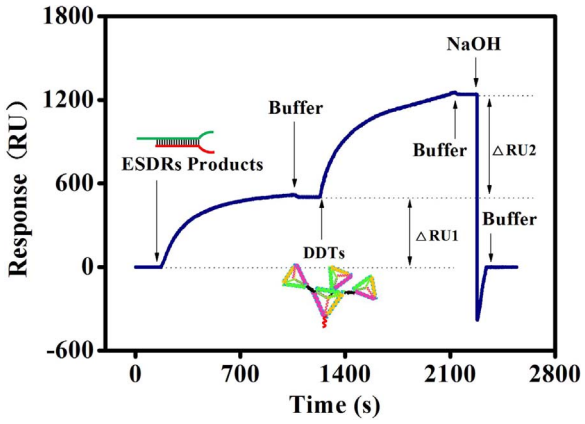

Fig. 1. Typical SPR sensorgram of ESDRs products hybridized with capture probes and DDTs cascade signal amplification.

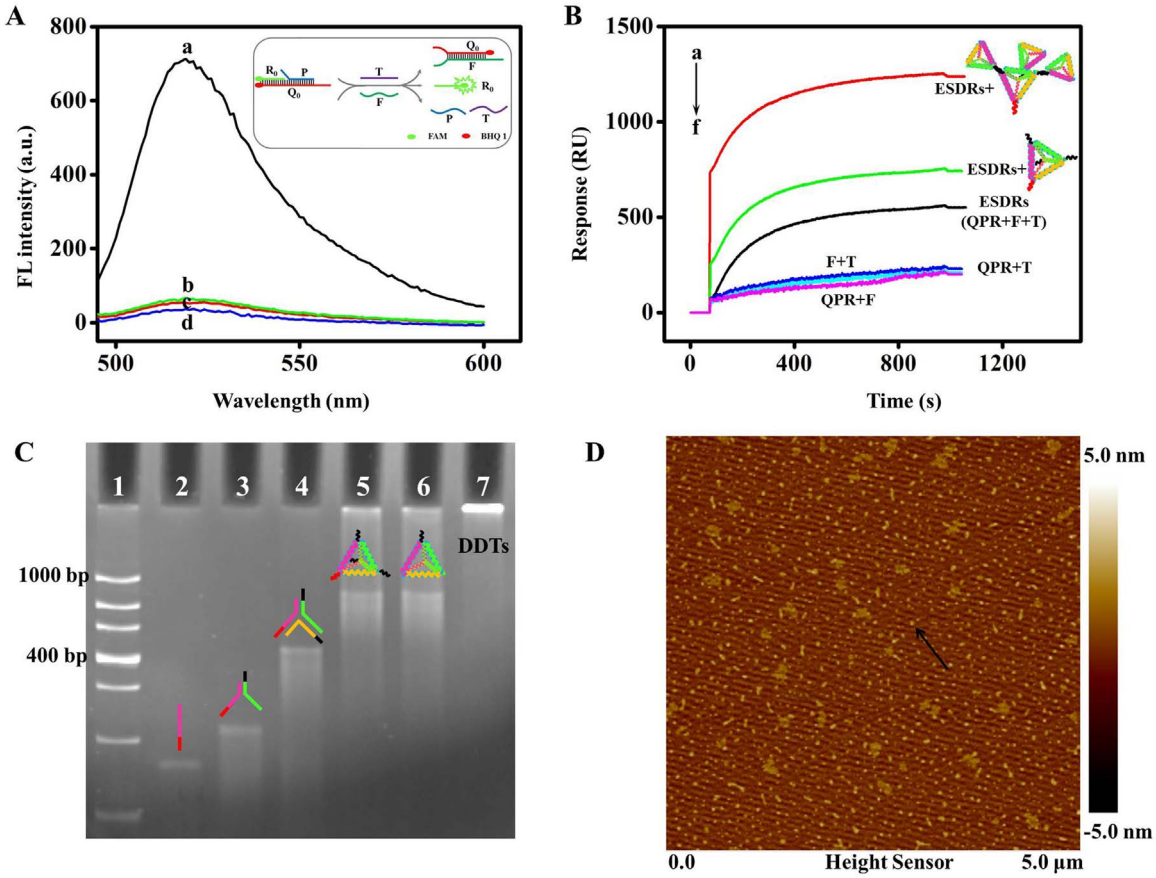

Fig. 2. (A) Typical fluorescence spectra of different experimental conditions of ESDRs with (a) complex QPR, target DNA and fuel strand F, (b) complex QPR and strand F, (c) complex QPR and target DNA, (d) only complex QPR. (B) SPR sensorgrams corresponding to ESDRs and DDTs (curve a), ESDRs and T_0 (curve b), only ESDRs (curve c), strand F and target DNA (curve d), complex QPR and target DNA (curve e), complex QPR and strand F (curve f). (C) Native polyacrylamide gel electrophoresis results of the products and sequences of DDTs. Lane 1: 1000 bp DNA ladder marker; Lanes 2, 3, 4: subsets assemblied by single strand, two strands and three strands DNA, respectively; Lane 5: DNA tetrahedron T_0; Lane 6: DNA tetrahedron T_1; Lane 7: DDTs. (D) AFM image for DNA tetrahedron T_0.

Meanwhile, a set of SPR experiments were performed to evaluate the feasibility of ESDRs amplification coupling DDTs nanostructure. As shown in Fig. 2B, having target DNA with ESDRs amplification, a high SPR signal of 550 RU was obtained because the formed DNA complexes on chip surface have high molecular weight, which enhanced the SPR signal obviously (curve c). The control experiments, excluding three-stranded complex QPR (curve d), fuel strand F (curve e) and target (curve f), showed only weak background signals with the values of 219, 208 and 197 RU, respectively. These results fell in line with those obtained by fluorescence method, confirming that the target DNA can trigger ESDRs with the help of strand F. To further verify the performance of DNA tetrahedron nanostructures on SPR signal amplification, we experimented monolayer DNA tetrahedron and DDTs nanostructures respectively. As shown in Fig. 2B, with monolayer DNA tetrahedron introduced, an SPR signal of 740 RU (curve b) was obtained which was much higher than that of only ESDRs (curve c). For comparison, when DDTs nanostructure was introduced, a notable growth in the SPR response (curve a) was observed with the value of 1200 RU. The results confirmed the successful coupling between ESDRs and DDTs nanostructure and the excellent performance of DDTs nanostructure on SPR platform. All the outcomes manifested here obviously demonstrated the feasibility of developed SPR biosensing platform for rapid detection of HIV-related DNA.

To verify the self-assembly of DNA tetrahedron and DDTs nanostructures, the products and sequences of DDTs were studied with a 8% native polyacrylamide gel electrophoresis (PAGE). As depicted in Fig. 2C, monolayer DNA tetrahedron (T_0/T_1) migrated more slowly than any other subsets assemblied by single strand, two strands or three strands DNA (Lane 2–6). The bands of T_0 and T_1 were observed at a similar position due to the resembled structure. With T_0 and T_1 combined into DDTs nanostructure, the band with the slowest migration was observed (Lane 7). The electrophoretic mobility of various DNA nanostructures took on degressive tendence according to the molecular weight, confirming the successful assembling of monolayer DNA tetrahedron and DDTs nanostructures.

AFM was further employed to directly observe the morphology of DNA tetrahedron nanostructure. The conformation of DNA tetrahedron was observed from Fig. 2D. The AFM results intuitively reflected the successful formation of DNA tetrahedron nanostructure.

3.3. Optimization of detection conditions

As depicted in Fig. 3, crucial experimental variables were researched to attain optimal sensing performance. The signal-to-noise ratio was utilized to assess the execution of the SPR biosensor. The binding process between capture probes and dsDNA F-Q could be strongly affected by the base number of binding site on strand Q. If the binding site of strand Q is excessively short, it is difficult for dsDNA F-Q to combine with capture probes. While if the binding site of strand Q is unnecessarily long, the formed dsDNA complex F-Q is unstable and the binding efficiency will be influenced as well. To obtain the best SPR response signal, the base number of binding site on strand Q were optimized. In this work, the binding site on strand Q was designed with different base number. The signal-to-noise ratio grew with the growing base number of the binding site up to 6, but tended to stable with the additional growing of base number (Fig. 3A). Thus, 6 base number was

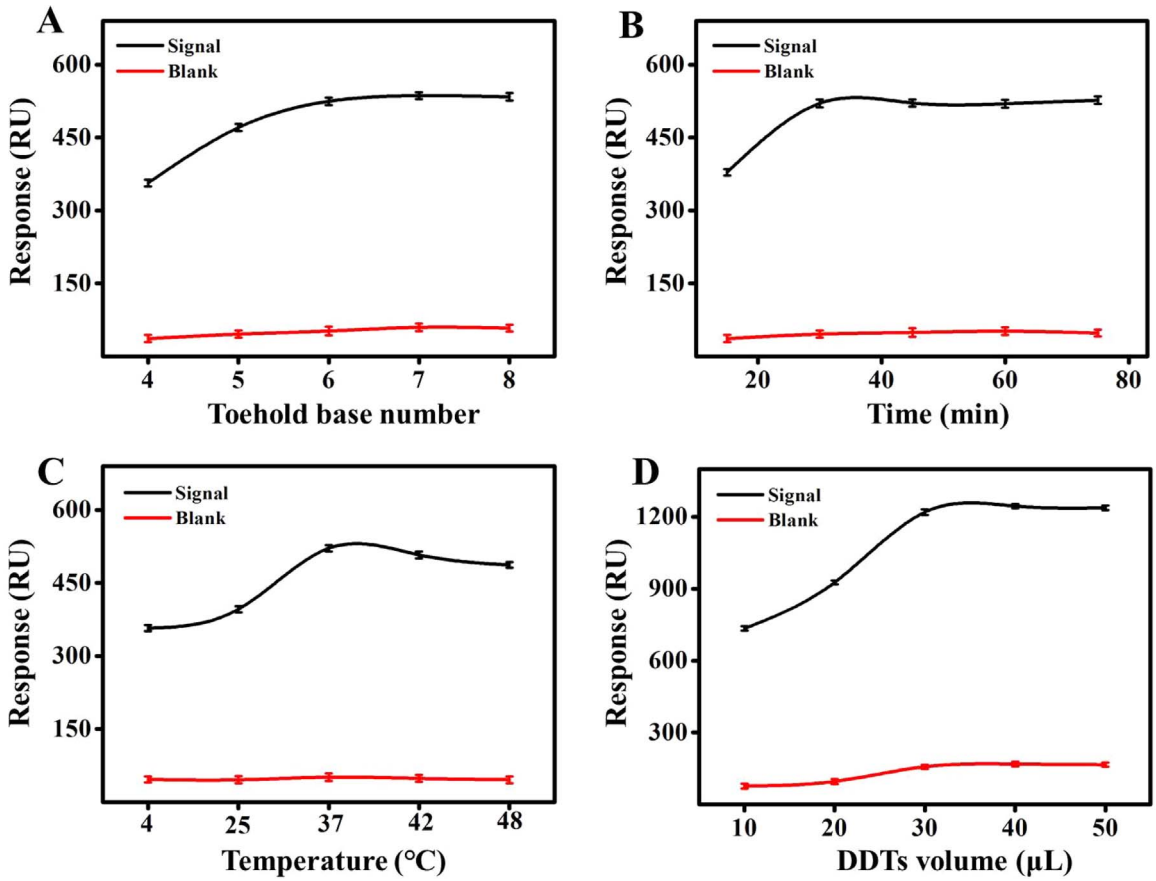

Fig. 3. Optimizations of experimental parameters: (A) evaluation of the base number of binding site on strand Q, (B) evaluation of the effect of incubating time of ESDRs, (C) evaluation of the effect of incubating temperature of ESDRs, (D) evaluation of the injection volume of DDTs.

selected as the optimal base number of the binding site.

Additionally, the incubating time and temperature of ESDRs were also optimized to improve sensing sensitivity. The influence of ESDRs incubating time on the signal-to-noise ratio was studied in Fig. 3B. As expected, the signal-to-noise ratio grew with the extension of reaction time and arrived at the platform at 30 min, showing the signal generated by target DNA arrived at the largest at 30 min and kept stable state. As a consequence, 30 min was chosen as the optimal reaction time. The reaction temperature was as well researched from 4 to 48 °C (Fig. 3C), and the maximum signal-to-noise ratio was attained at 37 °C. At low temperature, target DNA is unlikely to trigger ESDRs; at high temperature, the complexes QPR would disband leading to the increase of nonspecific signal. Therefore, 37 °C was chosen for the optimal reaction temperature.

Optimizing the injection volume of DDTs was also important for the rapid detection of HIV-related DNA. As depicted in Fig. 3D, the signal-to-noise ratio grew with the augment of the DDTs injection volume from 10 to 30 μL, since DDTs nanostructure can be attached to the SPR chip increasingly. With more DDTs nanostructure employed, the signal-to-noise ratio inclined to decrease, suggesting that the binding sites for DDTs reached the saturation state and overmuch DDTs could influence the signal. Hence, the injection volume of DDTs was fixed at 30 μL for the assay. The error bars in the diagram stand for the standard deviations in three different results for the parallel tests.

3.4. Analytical performance of target DNA detection

In order to assess the analysis capability of the designed SPR biosensor, different concentrations of target DNA were tested under optimal experiment conditions. As depicted in Fig. 4A, the SPR response signal grew proportionally with the concentration of target DNA. The calibration plots manifested a clear linear relationship between the response signals and the logarithm of target DNA concentrations in the scope of 1 pM to 150 nM (Fig. 4B). The resulting linear equation was Y(ΔRU) = 150.82 × lgC (nM) + 851.90 with the correlation coefficient of 0.9980. The limit of detection (LOD) was calculated to be 48 fM by putting 3 standard deviations of the response to blank sample into the linear equation, which was comparable with other methods on diverse biosensing platforms for HIV-related DNA detection (Table S2). In addition, the sensitivity of the developed method was compared with other nucleic acid detection methods on SPR biosensing platform in Table S3. The results indicated that the current strategy had superior analytical performance owing to the considerable amplification efficacy of ESDRs and extraordinary performance of DDTs. The established method not only had wide linear scope and low limit of detection, but also had simple and fast process because of the enzyme-free and label-free design. Furthermore, real-time fluorescent quantitative PCR (qPCR) was employed to verify the quantitative accuracy. The plots of the cycle thresholds (Ct) vs. the logarithm of target DNA concentration showed a strong linear relationship in the range from 1 pM to 1 nM, with the correlation coefficient of −0.9914 (Fig. S2A). When comparing the results of two assays using regression analysis, the plots of Ct obtained with the qPCR assay vs that of SPR signals obtained with the established biosensor give a R^2 value of 0.991 (Fig. S2B), confirming the good consistency of two methods.

3.5. Specificity, duplicability and reusability of the strategy

To evaluate the selectivity of the developed SPR method, four distinct control DNA sequences, including target DNA, single-base mismatch target (SM), double-base mismatch target (DM), as well as non-complementary sequence (NC) were used. As shown in Fig. 5, the

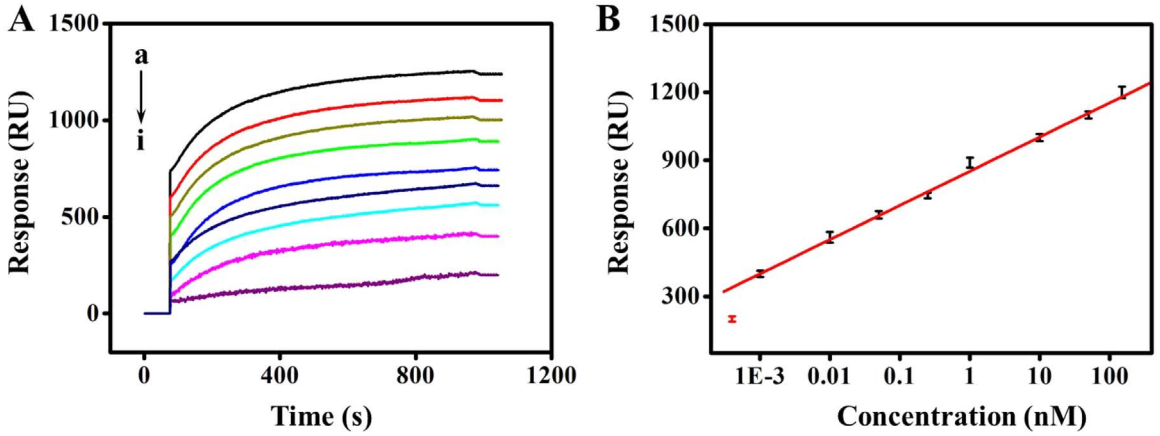

Fig. 4. (A) SPR sensorgrams for detection of HIV-related DNA at 150, 50, 10, 1, 0.25, 0.05, 0.01, 0.001, 0 nM (from a to i), (B) The calibration curve of the designed strategy for HIV-related DNA detection. The error bars represent the standard deviations calculated from three different spots.

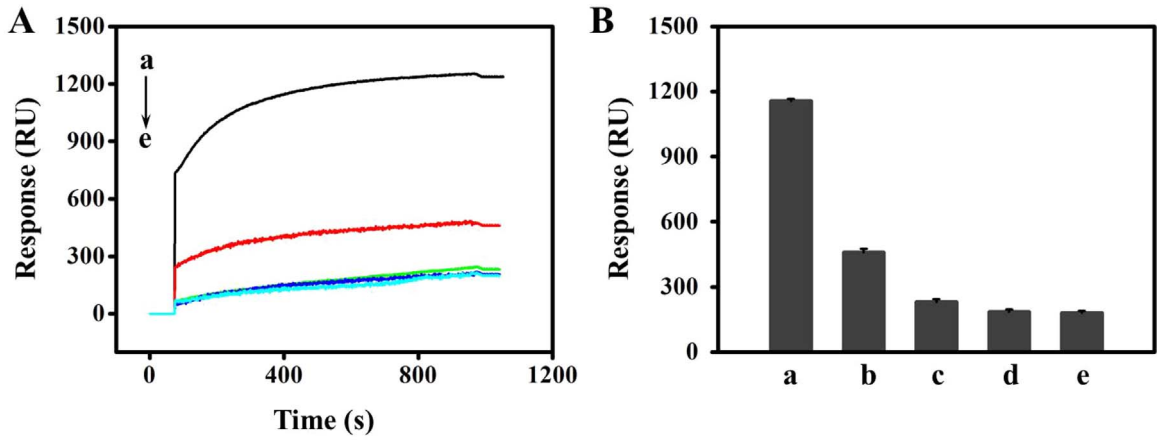

Fig. 5. (A) SPR sensorgrams and (B) SPR signal response respectively corresponding to 50 nM of HIV-related DNA (a), single-base mismatched oligonucleotides (b), two-base mismatched oligonucleotides (c), non-complementary oligonucleotides (d), and blank (e).

response signals of DM and NC were approximate to signals of blank. However, a notable increase in the response signal was observed together with target DNA. The response of target DNA was approximately 2.5 times as that of SM and 6 times as that of DM and NC. These outcomes showed that this method displayed remarkable specificity for the determination of target DNA.

Moreover, the same target DNA sample (10 nM) had been measured five times to verify the duplicability of intra-assay. As shown in Table S4, the variation coefficient was 0.5% indicating good duplicability for intra-assay. In addition, the target DNA at 10 pM and 10 nM with ten duplicates were measured for researching the duplicability of the prepared biosensor for inter-assay. Consequently, the variation coefficients for the concentrations were approximately 1.6% and 1.3% (Table S5), respectively, demonstrating good fabrication duplicability. To further explore the reutilization of the biosensor, repeated regenerations were implemented on the same chip. After about 100 times regenerations, the SPR response signal of 1 nM target DNA retained 91.5% of the initial signal, implying the same sensor chip can be used again more than 100 times without obvious degradation of the analysis capability.

3.6. Recovery test

To assess the usability and dependability of the developed method in complicated biological environment, the recovery tests were performed using C57 wild type mice tail total DNA as an example (taking laboratory biosafety into account, samples from AIDS patients had not been used). The total DNA sample was dissolved to 400 ng μL^{-1} with ultrapure water, and 2.5 μL total DNA sample was diluted to 100 μL with ESDRs buffer (1 μg in total) for further measurement. Then, different amounts of target DNA were spiked into 1 μg C57 wild type mice tail total DNA for the assay. The recoveries were 96–108% from 10 pM to 100 nM (Table S6), indicating that the developed method could be a probable approach for target DNA analysis in real samples.

4. Conclusion

To conclude, an enzyme-free and label-free SPR biosensing strategy has been developed for HIV-related DNA detection by ESDRs and DDTs cascade amplification. The developed SPR biosensing strategy can be used for the detection of target DNA down to femtomolar level with high specificity, and has been applied to complex matrices. The excellent performance can be attributed to the perfect combination of hairpin probe, ESDRs circuit and DDTs nanostructure on SPR biosensing platform. Also, the proposed method showed prominent advantages including simple process, good stability, high repeatability, fast speed and low cost. More importantly, because the sequence design of ESDRs is flexible, the SPR biosensing strategy based on dynamic and structural DNA nanodevices can be extended to detect other targets just by changing the sequences of ESDRs. Taken together, the developed strategy has large application prospect in rapid and early clinical diagnosis of HIV infection and other genetic disease.

Acknowledgements

This work was funded by the National Natural Science Foundation of China (81371904 and 81572080), the Achievement Transfer Project

of Institutions of Higher Education in Chongqing (KJZH14205), the Special Project for Social Livelihood and Technological Innovation of Chongqing (cstc2016shmszx130043), the Research Innovation Project for Post Graduate of Chongqing Municipal (CYS16139 and CYS16135).

Appendix A. Supplementary material

Supplementary data associated with this article can be found in the online version at doi:10.1016/j.bios.2017.08.042.

References

Avettand-Fenoel, V., Chaix, M.L., Blanche, S., Burgard, M., Floch, C., Toure, K., Allemon, M.C., Warszawski, J., Rouzioux, C., 2009. J. Med. Virol. 81, 217–223.
De la Rica, R., Stevens, M.M., 2012. Nat. Nanotechnol. 7, 821–824.
Ding, X., Cheng, W., Li, Y., Wu, J., Li, X., Cheng, Q., Ding, S., 2017. Biosens. Bioelectron. 87, 345–351.
Douglas, S.M., Chou, J.J., Shih, W.M., 2007. Proc. Natl. Acad. Sci. USA 104, 6644–6648.
Feng, Q.M., Guo, Y.H., Xu, J.J., Chen, H., 2017. ACS Appl. Mater. Interfaces 9, 17637–17644.
Girardi, E., Sabin, C.A., Monforte, A.D., 2007. J. Acquir. Immune Defic. Syndr. 46 (Suppl 1), S3–S8.
Goodman, R.P., Schaap, I.A., Tardin, C.F., Erben, C.M., Berry, R.M., Schmidt, C.F., Turberfield, A.J., 2005. Science 310, 1661–1665.
Hao, K., He, Y., Lu, H., Pu, S., Zhang, Y., Dong, H., Zhang, X., 2017. Anal. Chim. Acta 954, 114–120.
He, L., Lu, D.Q., Liang, H., Xie, S., Luo, C., Hu, M., Xu, L., Zhang, X., Tan, W., 2017. ACS Nano 11, 4060–4066.
Li, C., Wu, D., Hu, X., Xiang, Y., Shu, Y., Li, G., 2016a. Anal. Chem. 88, 7583–7590.
Li, J., Lei, P., Ding, S., Zhang, Y., Yang, J., Cheng, Q., Yan, Y., 2016b. Biosens. Bioelectron. 77, 435–441.
Li, X., Cheng, W., Li, D., Wu, J., Ding, X., Cheng, Q., Ding, S., 2016c. Biosens. Bioelectron. 80, 98–104.
Li, X., Li, D., Zhou, W., Chai, Y., Yuan, R., Xiang, Y., 2015. Chem. Commun. 51, 11084–11087.
Li, Z., Zhao, B., Wang, D., Wen, Y., Liu, G., Dong, H., Song, S., Fan, C., 2014. ACS Appl. Mater. Interfaces 6, 17944–17953.
Lin, M., Song, P., Zhou, G., Zuo, X., Aldalbahi, A., Lou, X., Shi, J., Fan, C., 2016. Nat. Protoc. 11, 1244–1263.
Lin, M., Wang, J., Zhou, G., Wang, J., Wu, N., Lu, J., Gao, J., Chen, X., Shi, J., Zuo, X., Fan, C., 2015. Angew. Chem. Int. Ed. Engl. 54, 2151–2155.
Liu, S., Su, W., Li, Z., Ding, X., 2015. Biosens. Bioelectron. 71, 57–61.
Long, Y., Zhou, C., Wang, C., Cai, H., Yin, C., Yang, Q., Xiao, D., 2016. Sci. Rep. 6, 23949.
Lv, Y., Cui, L., Peng, R., Zhao, Z., Qiu, L., Chen, H., Jin, C., Zhang, X.B., Tan, W., 2015. Anal. Chem. 87, 11714–11720.
Mao, X., Simon, A.J., Pei, H., Shi, J., Li, J., Huang, Q., Plaxco, K.W., Fan, C., 2016. Chem. Sci. 7, 1200–1204.
Miao, Y.B., Ren, H.X., Gan, N., Zhou, Y., Cao, Y., Li, T., Chen, Y., 2016. Biosens. Bioelectron. 86, 477–483.
Pei, H., Li, F., Wan, Y., Wei, M., Liu, H., Su, Y., Chen, N., Huang, Q., Fan, C., 2012. J. Am. Chem. Soc. 134, 11876–11879.
Qaddare, S.H., Salimi, A., 2017. Biosens. Bioelectron. 89, 773–780.
Shi, K., Dou, B., Yang, C., Chai, Y., Yuan, R., Xiang, Y., 2015. Anal. Chem. 87, 8578–8583.
Wang, Q., Li, Q., Yang, X., Wang, K., Du, S., Zhang, H., Nie, Y., 2016. Biosens. Bioelectron. 77, 1001–1007.
Wang, Y., Bai, X., Wen, W., Zhang, X., Wang, S., 2015. ACS Appl. Mater. Interfaces 7, 18872–18879.
Wu, H., Liu, Y., Wang, H., Wu, J., Zhu, F., Zou, P., 2016. Biosens. Bioelectron. 81, 303–308.
Wu, L., Zhang, Q., Su, L., Huang, M., Zhao, J., Yang, M., 2007. Sens. Actuators B 122, 243–252.
Wu, Y., Zhang, D.Y., Yin, P., Vollmer, F., 2014. Small 10, 2067–2076.
Xiang, Y., Zhu, X., Huang, Q., Zheng, J., Fu, W., 2015. Biosens. Bioelectron. 66, 512–519.
Xie, S., Dong, Y., Yuan, Y., Chai, Y., Yuan, R., 2016. Anal. Chem. 88, 5218–5224.
Yao, G.H., Liang, R.P., Yu, X.D., Huang, C.F., Zhang, L., Qiu, J.D., 2015. Anal. Chem. 87, 929–936.
Yuan, P.X., Deng, S.Y., Zheng, C.Y., Cosnier, S., Shan, D., 2017. Biosens. Bioelectron. 97, 1–7.
Zhang, D.Y., Seelig, G., 2011. Nat. Chem. 3, 103–113.
Zhou, L., Huang, J., Yu, B., Liu, Y., You, T., 2015. ACS Appl. Mater. Interfaces 7, 24438–24445.
Zhou, W., Gong, X., Xiang, Y., Yuan, R., Chai, Y., 2014. Biosens. Bioelectron. 55, 220–224.
Zhu, G., Hu, R., Zhao, Z., Chen, Z., Zhang, X., Tan, W., 2013. J. Am. Chem. Soc. 135, 16438–16445.